Dye-Labeled Silver Nanoshell−Bright Particle

Jian Zhang, Ignacy Gryczynski, Zygmunt Gryczynski, and Joseph R. Lakowicz*

Center for Fluorescence Spectroscopy, University of Maryland School of Medicine, Department of Biochemistry and Molecular Biology, 725 West Lombard Street, Baltimore, Maryland 21201

Received: December 2, 2005; In Final Form: March 6, 2006

Silica beads with *average* diameters of 40−600 nm were prepared, and $Ru(bpy)_3^{2+}$ complexes were incorporated into the beads. These beads were coated by silver layer by layer to generate porous but continuous metal nanoshells. The thicknesses of these metal shells were 5−50 nm. The emission band from the dyes in the silica cores was more narrow and the intensity was enhanced with growth of silver shell thickness due to coupling of the emission light from $Ru(bpy)_3^{2+}$ in the cores with the metal plasmon from the silver shells. The enhancement of emission intensity was also dependent on the size of the silica core, showing that the enhancement efficiency decreased with an increase in the size of the silica beads. Lifetime measurements support the coupling mechanism between the dye and metal shell. This study can be used to develop novel dye-labeled metal particles with bright and narrow emission bands.

Introduction

Fluorescence is known to enhance when fluorophores are localized near a metal surface.[1] Recently, there has been increased interest in metallic particles as next generation nanoscale superstructures for use in chemical and biological sensing.[2] Hence, it is important to develop highly sensitive sensing techniques for metal particles using the fluorescence enhancement principle. Such metal-enhanced fluorescence (MEF) is attributed to a coupling of dye with an electromagnetic (EM) field near the metal particle.[3] The EM field is regarded to be dependent on the features of the metal particle (metal species, size, shape, etc.).[4−6] Generally, dye molecules can be simply bound onto the metallic particle. However, our experiments reveal that fluorescence is even more enhanced when those dye-bound particles are coupled to each other.[7] In other words, the emission can be enhanced more efficiently when the dyes are localized in a cumulative EM field, where the field intensity is extremely strong. Hence, if a sensing nanodevice is designed as a metal shell instead of a core, the fluorescence emission of the dyes localized inside the shell is expected to enhance more efficiently to create a bright and photostable probe by combining fluorophores with plasmon resonant particles (PRPs).

Although there are many complexities arising when a fluorophore is placed very close to the metal including to its chemical structure, orientation, and other unknown factors, some limited calculations are available for spherical silver nanoshells.[8] These calculations included the loss of energy as heat during transfer of energy across the metal shell in both directions and also provided a reliable estimation of the emission intensity. Even after this attenuation, the emission from a single fluorophore is expected to be 10 to 100-fold higher when contained in a nanoshell. Meanwhile, besides the cross-interaction between the dye and metal plasmon, there are other factors that can result in more efficient emission enhancement. The shorter lifetime of the fluorophore in the metal shell results in less time for photochemistry while in the excited state and thus more excitation−emission cycles prior to photobleaching.[1a,b] The metal shell may prevent the entrance of oxygen and other species to some extension that react with the fluorophore and thus protect the fluorophore from photochemical reactions. In addition, one single nanoshell may contain tens of dye molecules, so that we can image that one nanoshell 100 times brighter than one dye under the same conditions. Meanwhile, it is known that the EM field within a metal shell is uniform for the small core size,[8] suggesting that all the dye molecules in this shell may be equally enhanced irrespective of location within the nanoshell. These considerations suggest that fluorophores encapsulated in metal nanoshells can be bright and photostable particles for single molecule detection and imaging.

It is known that the silica beads can work as markers in biological sensing when they are dye-labeled.[9] They are also utilized as the cores to coat with the metal nanoshells to create metal core−shell structures.[10−12] Therefore, the silica beads were used as the core for the metal shell in this study. The silica beads with different sizes were synthesized by the Stöber method and labeled by the $Ru(bpy)_3^{2+}$ complex, a photostable dye used for chemical and biological research.[13] The dye was physically adsorbed into the silica bead during the bead formation.[14] The surface of the dye-labeled silica bead was aminated using 3-aminopropyltrimethoxy silane, and then, a silver nanoshell was coated onto the silica bead layer by layer to control the metal thickness. The correlation between emission spectral change and the thickness of the silver shell was investigated in this study. The dye-labeled silica bead was also made in different sizes to study the dependence of emission spectral change on the silica core size for the silver nanoshell.

Experimental Section

All reagents and spectroscopic grade solvents were used as received from Fisher or Sigima-Aldrich. Nanopure water (>18.0 MΩ) purified using a Millipore Milli-Q gradient system was used in all of the experiments.

Preparation of Dye-Labeled Silica Beads. Monodispersed silica beads were prepared using the Stöber method by codissolving 1.0×10^{-6} M $Ru(bpy)_3^{2+}ClO_4$ and 1.4×10^{-2} M tetraethyl orthosilicate in 50 mL of ethanol. Ammonia (1, 3, 5, 10, and 20 mL of 30% NH_3, respectively) was then added

10.1021/jp057032z CCC: $33.50
Published on Web 04/14/2006

SCHEME 1: Preparation of $Ru(bpy)_3^{2+}$-Labeled Silica Bead and Silver Nanoshell in a Particle-Seeding and Then Layer-by-Layer Growth Model

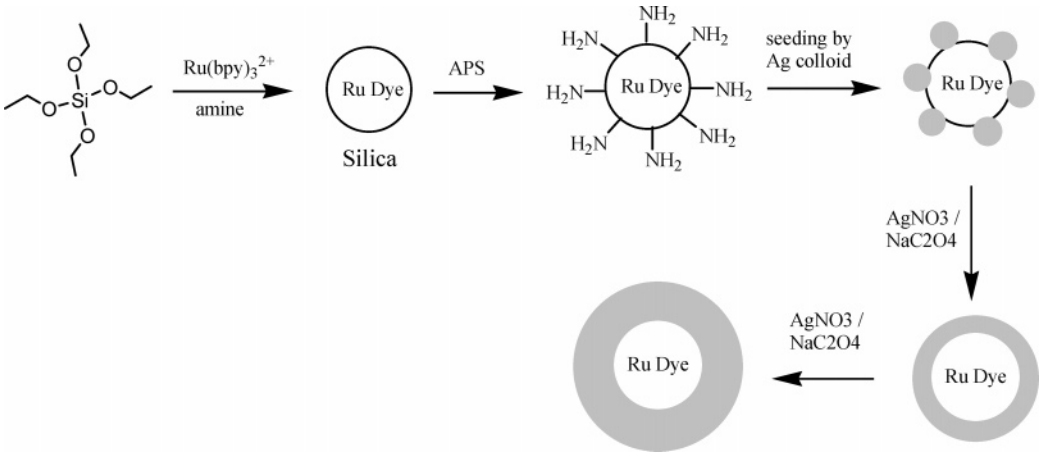

dropwise under vigorous stirring (Scheme 1).[15] The solution was kept stirring overnight. The solution became muddy due to the formation of silica beads. The mixture was centrifuged to remove the ethanol, and the residual was washed thoroughly with ethanol. The beads were redispersed in 50 mL of ethanol and aminated by adding 10 μL of 3-aminopropyltrimethoxy silane with continuous stirring for 5 h. These aminated beads were centrifuged, washed with ethanol, and then dispersed in 10 mL of water.

Preparation of Metal Nanoshells. Silver colloids (*average* diameter = 20 nm), which were prepared by reduction of silver nitrate (10 mM) using trisodium citrate (20 mM) in water at 95 °C.[2a] A 1 mL portion of aminated silica bead solution was added into 50 mL of silver colloid solution with continuous stirring for 2 h to conjugate these silver colloids onto silica beads. The conjugates were then noted to precipitate from solution. The water solution was removed by centrifugation, and the residue was redispersed in water.[9c] The silver shells were grown on the colloid-seeded beads by adding the conjugate solution into 50 mL of $AgNO_3$ (10 mM) and sodium citrate (20 mM) water solution, and the reduction occurred at 80 °C. The silver shells were recovered by centrifugation to remove water solution and then dispersed in water to repeat the operation of growing the silver shell (Scheme 1). The solution amount of silver nitrate and sodium citrate was adjusted slightly in each operation to control the growth of silver shell.

Spectra Measurements. Absorption spectra were monitored with a Hewlett-Packard 8453 spectrophotometer. Fluorescence spectra were recorded with a Cary Eclipse fluorescence spectrophotometer. Lifetimes were measured by single photon counting using a PicoQuant modular fluorescence lifetime spectrometer (Fluo Time 100) with a PicoQuant 460−480 nm LED (LDH-P-L-470) as the light source. The samples were in a 1 cm cell with absorbance at 0.2−0.5. The collected data were analyzed using PicoQuant Fluofit 3.3 software. Transmission electron micrographs (TEMs) were taken with a side-entry Philips electron microscope at 120 keV. Samples were cast from water solutions onto standard carbon-coated (200−300 Å) Formvar films on copper grids (200 mesh) by placing a droplet of a 1 mg/mL aqueous sample solution on the grids. The size distribution of the metal core was analyzed with Scion Image Beta Release 2, counting at least 200 particles.

Results and Discussion

The silica beads were prepared using the Stöber method, and the sizes of these beads were controlled by the amount of ammonium in the preparation. The silica beads were identified from transmission electron micrographs (TEMs). It was shown that the beads became large with an increase in the quantity of ammonium (Figure 1a and b, all data were listed in Table 1). On the basis of the emission spectral change from $Ru(bpy)_3^{2+}$ in solution before and after the bead formation, we suggest that most of the $Ru(bpy)_3^{2+}$ molecules in the initial solution were incorporated into the silica beads, and the concentration of $Ru(bpy)_3^{2+}$ in the silica beads was estimated to be near 1×10^{-4} M (Table 1), almost independent of the size of the silica beads. According to the bead size, the concentration was stated as an average number of dye molecules per bead (Table 1). This concentration is not high, so the self-quenching between the dyes was negligible in the silica bead. We found that there was almost no $Ru(bpy)_3^{2+}$ leaching to solution even when the dye-labeled beads were stored in water for a week as well as during the operations of shell growth and purification as discussed later, implying that the absorption of $Ru(bpy)_3^{2+}$ in the silica matrix was strong.

TABLE 1: Correlation of Ammonium Amount Used in the Preparation of Dye-Labeled Silica Beads and Their Properties

ammonium quantity (mL)	1	3	5	10	20
average diameter of bead (nm)	40	100	200	400	600
average dye number per bead	4	30	200	1500	5000

The silica beads were aminated using 3-aminopropyltrimethoxy silane and then conjugated by citrate-protected silver colloids. Such conjugation was verified by the TEM image shown in Figure 1c. These metal colloids on the silica beads acted as seeds for a smooth growth of metal shells.[9c] The metal shells on silica beads were grown layer by layer by chemical reduction of silver nitrate and verified by TEM images. The thickness of the metal shell was estimated by subtracting the silica bead diameter from the total diameter of the shell. Besides the first layer, which was about 5 nm, each repetitive silver accumulative operation could lead to about a 10 nm thick metal shell accumulation on the silica bead under the current conditions. The final thickness of the metal shell reached 55 nm after six layers of silver deposition. Compared with the consuming quantity of silver salt in the reduction, the growth of the silver shell was almost 2 times thicker, implying that the forming metal shells might be porous and continuous. This viewpoint was also verified by their TEM images (Figure 1d), on which the margin of metal shell was quite rough.

The dye-labeled silica beads displayed a strong scattering even though it was an orange color, so the absorption of the dye is

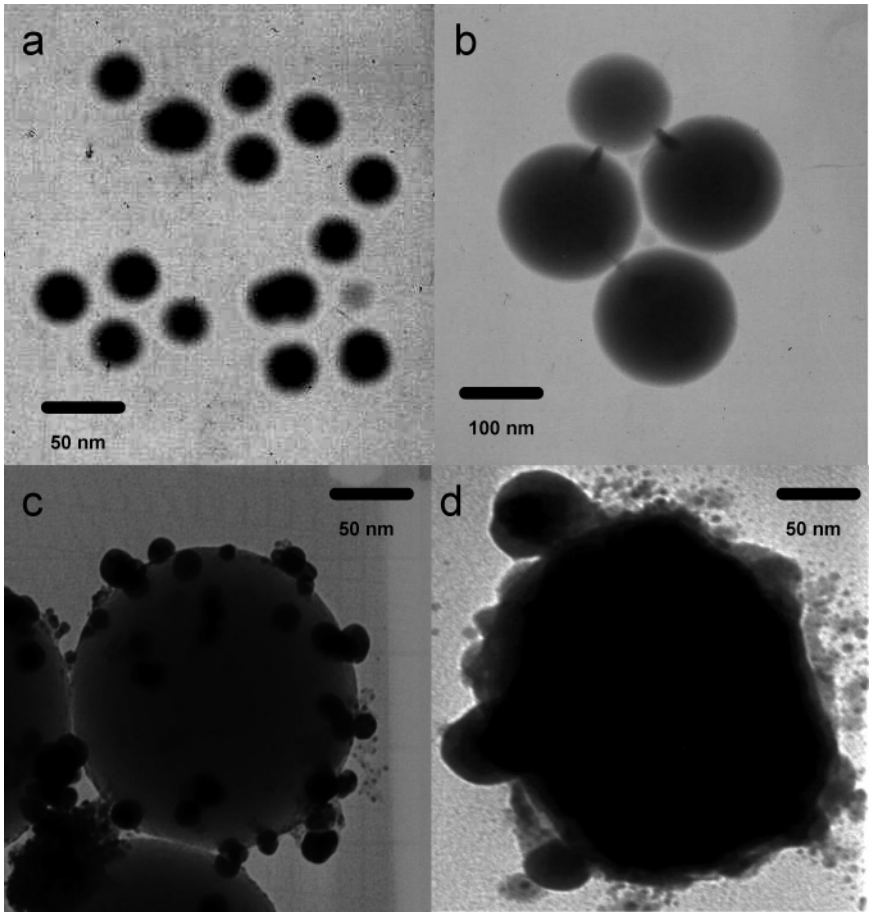

Figure 1. TEM images for (a) silica bead made by 1 mL of ammonium, (b) silica bead made by 10 mL of ammonium, (c) silver particle seeded bead, and (d) silver nanoshells with silica cores made by 5 mL of ammonium and a metal shell thickness of 30 nm.

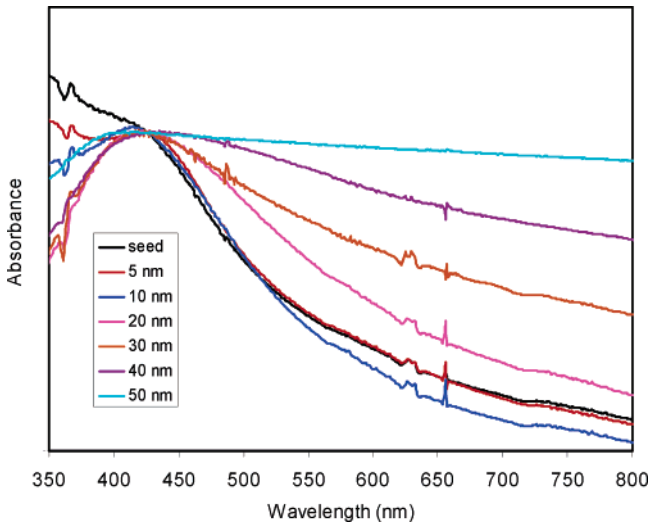

Figure 2. Absorbance spectrum of silver shells with 200 nm diameter silica cores but growing metal shells.

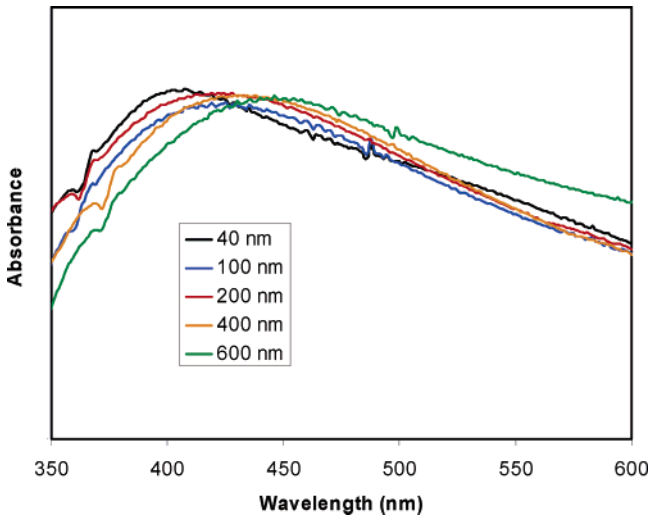

Figure 3. Absorbance spectra of silver shells with 30 nm thick metal shells but different size silica cores.

barely present on the extinction profile. When the silver colloids were seeded onto the silica beads, a metal plasmon absorbance rose near 400 nm (Figure 2), which was from the conjugated metal particles. The plasmon absorbance band became stronger and broadened with the silver shell growth, but the wavelength did not have significant shifting. This result was consistent with the observation from Liu et al.[9c] The plasmon wavelength from the silver nanoshell was red-shifted from 400 to 450 nm when the size of the silica beads was increased from 40 to 600 nm. These shifting values are much shorter than those theoretically predicted,[8] which is principally due to the porous property of silver shell as well as the dielectric property of silica bead.

The dye-labeled silica beads displayed an emission maximum at 605 nm upon excitation at 450 nm, 7 nm blue-shifted from free dye in water. It was interesting to notice that the emission band become narrower when the silver shell was deposited on the silica bead (taking an example for the diameter of silica bead =200 nm in Figure 4). This narrowness was not observed clearly when the beads were only seeded by silver colloids or coated by thin metal shells but became obvious with growth of

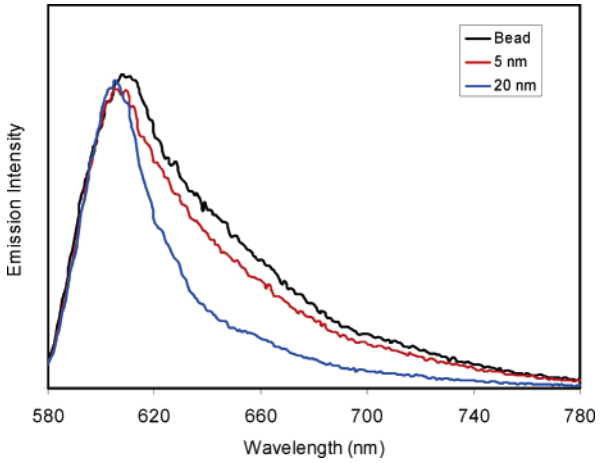

Figure 4. Emission spectra of $Ru(bpy)_3^{2+}$-labeled silica beads (diameter 200 nm) and their silver nanoshells with different metal thicknesses upon excitation at 450 nm. The emission band was more narrow when the metal shell became thick.

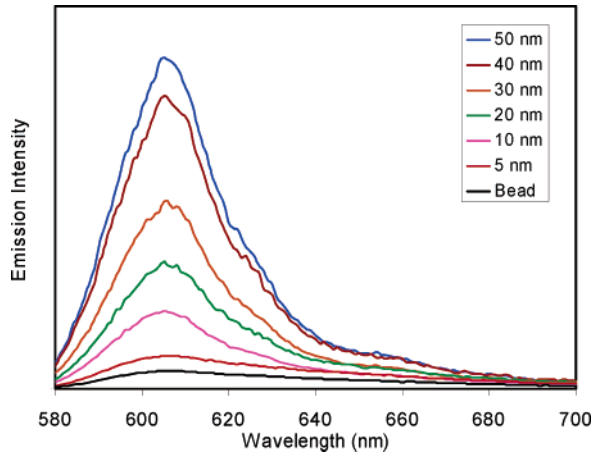

Figure 5. Dependence of emission spectrum of dye-labeled silver shells with silica beads (diameter 200 nm) on metal thickness upon excitation at 450 nm. The $Ru(bpy)_3^{2+}$ concentrations were normalized to 4.4×10^{-7} M in solution. The control was done removing the four-layer silver shell by sodium cyanide in solution.

the silver shell. The narrower emission spectra for the dye-labeled metal nanoshell have been predicted by theoretical calculation.[16] We believe herein that the narrowed emission may be due to a coupling of the excitation energy of the dye with the surface plasmon in the metal shell. The observed emission is the result of plasmon radiating light into the far field. For a thin shell, the coupling is weak so the narrowness is not obvious. With the metal shell growth, the thick shell is more suitable for coupling between exited fluorophore and surface plasmon. This observation, we believe, is an important discovery in fluorophore−metal coupling, related to radiative decay engineering (RDE)[1a,b] and surface plasmon-coupled emission (SPCE).[18] When the silver shell was removed by dissolution with sodium cyanide in solution, the emission band reverted to that from the dye-labeled bead without a metal shell, implying that the narrowness of the emission spectrum can indeed be attributed to the presence of the metal shell.

Using the same concentration of dye-labeled bead, we observed that the emission spectrum became stronger with shell growth (taking an example for the diameter of silica bead = 200 nm in Figure 5). The enhancement efficiency, estimated to be a ratio of the intensity from the silver shell over that of the silica bead at the same bead concentration, was plotted against (TEM-identified) shell thickness (Figure 6). It was shown that,

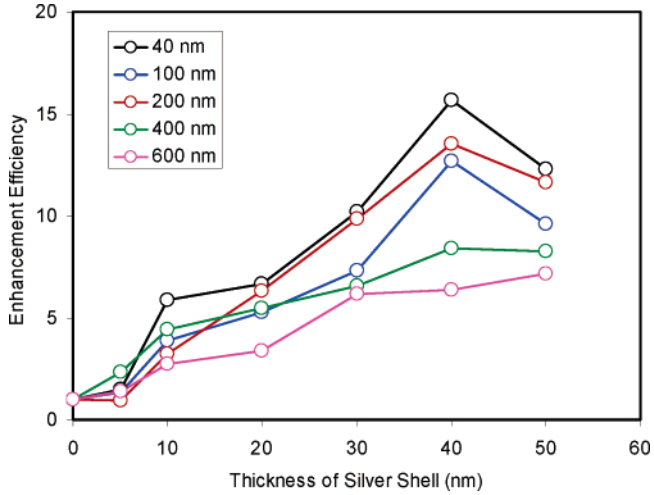

Figure 6. Dependences of the emission enhancement efficiency of silver nanoshells with different silica core beads on the silver shell thickness.

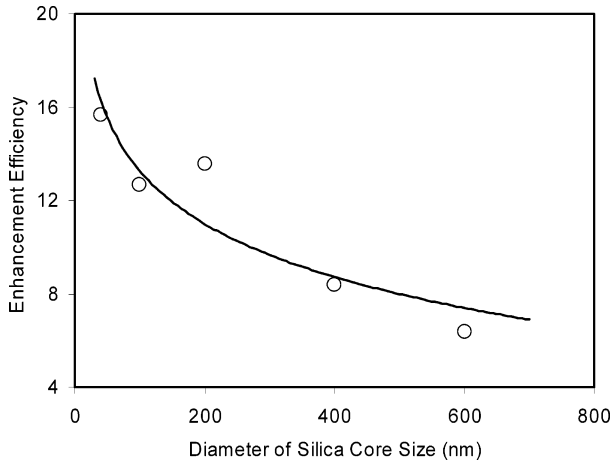

Figure 7. Dependences of maximal emission enhancement efficiency for the silver shells on the silica bead sizes.

for all five different sized silica beads, the emission intensity could not be enhanced efficiently at a thin metal shell below 5 nm but then rose with an increase of metal shell thickness. The enhancement reached saturates at 40 nm. The emission spectrum began to decrease slightly when the shell thickness was over 40 nm. The maximum enhancement efficiency was 15.7 times for the smallest silica bead coated by a 40 nm thick metal shell. This value can be compared with theoretical prediction of 30-fold enhancement for rhodamine 6G in an optimal size and thickness of silver nanocavity.[16b] Also, it was shown that the maximum enhancement efficiency was decreased with an increase of silica core size (Figure 7).

Emission enhancement is regarded to come from the EM enhancement mechanism, in which plasmon excitation from the metal particle creates an enhanced EM field nearby.[1,4] For the small metal shells (10 nm size), the EM field stays uniform inside the cavity.[8] However, for the large metal shells in this study, the finite wavelength effect leads to depolarization, and thus, the field inside the shell is heterogeneous. According to a discrete dipole approximation (DDA) model suggested by Schatz and Hupp, the maximal EM enhancement field occurs close to the shell surface along the *x*-axis.[8a] We expect that the volume of efficient EM enhancement field becomes relatively smaller compared with the whole interior volume of the nanocavity with increasing size of the silica core. It means that the number of dye molecules localized in the efficient EM enhancement field

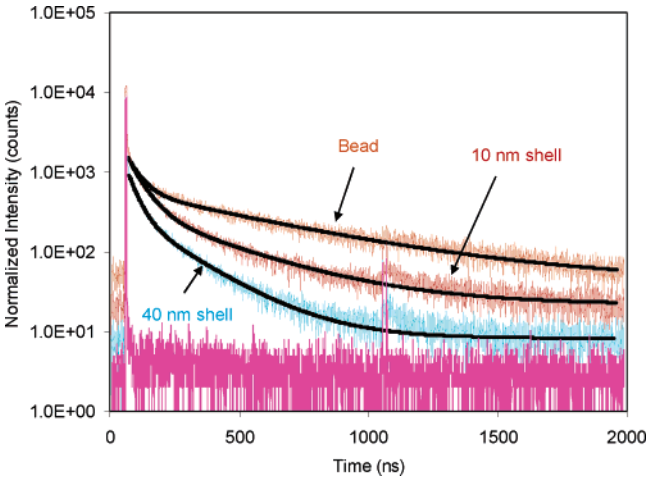

Figure 8. Emission decay curves fits for the $Ru(bpy)_3^{2+}$ in bare silica bead, 10 nm thick silver shell, and 40 nm thick silver shells on the silica beads with an average diameter of 200 nm.

was decreased with increasing size of the silica core, so that the maximal enhancement efficiency was shown to reduce with an increase of silica bead size in this study. Forthermore, it is also expected that the efficient EM enhancement field becomes larger and stronger with an increase of metal shell thickness so that the enhancement efficiency increases with the metal shell thickness.[8] When the metal shell creates a saturated efficient EM enhancement field in the cavity, a thicker metal shell is only able to block the emission of dye due to strong absorption at excitation and emission wavelengths so that the enhancement efficiency decreases after a maximal value.

Different from some polymer matrixes that are composed of hydrophilic/hydrophobic regions such as Nafion,[18] the silica beads are quite hydrophilic gels. When the $Ru(bpy)_3^{2+}$ are physically adsorbed into the silica beads, they are expected to disperse homogeneously into the whole beads. Because the silica beads were relatively large, it was suggested that only a portion of dyes localized in the efficient EM field were enhanced but the others were not. The shell in this study exhibited strong emission enhancement, implying that the enhancement of emission from the dyes in the "hot" region should be much more efficient than the apparent value. Compared with the 1 order of magnitude enhancement for the dye localized on the outside of the metal particle, the interior enhancement is stronger due to a more intensive interior electromagnetic field.

Emission enhancement on metal surfaces is believed to occur through an increase of the intrinsic decay rate for the fluorophore near the metal surface. As a result, lifetime is an important parameter through which to evaluate this mechanism.[3] To our knowledge, there are no publications to describe the different hydrophilic/hydrophobic regions in the silica bead. Intensity decays were fit with a double-exponential function model for the $Ru(bpy)_3^{2+}$ in the silica beads in the absence or presence of silver shells in this study (Figure 8), and some data are listed in Table 2. It was shown that all *chi* values ranged between 1.1 and 1.5, indicating that the double-exponential function fit well. The *average* lifetime of $Ru(bpy)_3^{2+}$ in beads was 497 ns, longer than that in water (382 ns), which was ascribed to the immobilization of $Ru(bpy)_3^{2+}$ in the solid matrix. After coating the silver shell on the silica bead, the lifetime decreased progressively with shell growth, which could be shown in Figure 8. The shortest lifetime obtained was 131 ns for a 40 nm thick shell on the 200 nm silica bead, which was only about $^1/_4$ of that from bare beads. The observed shortest lifetime also correlates to the strongest intensity enhancement for the silver shell sample, implying that the increase of the intrinsic decay rate of the fluorophore near the metal surface was an important factor in controlling emission enhancement. The silver shell on the larger silica shell resulted in a longer lifetime, consistent with the decreased emission intensity. It is known that the decrease in lifetime can lead to the increased photostability as measured in terms of excitation−radiation cycles.[3] This suggests that the number of detectable dyes may increase on the order of 50-fold (4 × 13.5) for the particle as compared to a bare bead.

TABLE 2: Lifetime Data Obtained Using the Double-Exponential Model for the $Ru(bpy)_3^{2+}$ Incorporated into Silica Beads and Then Coating with Silver Shells

sample	τ_i (ns)	α_i	$\langle\tau\rangle$ (ns)	χ_R^2
$Ru(bpy)_3^{2+}$ in water	382.1	1.0	382.1	1.32
$Ru(bpy)_3^{2+}$ in 100 nm silica bead	49.24	0.647	497.3	1.20
	568.4	0.353		
200 nm silica bead/10 nm silver	56.73	0.642	464.9	1.15
	541.6	0.358		
200 nm silica bead/30 nm silver	28.20	0.700	147.8	1.43
	189.0	0.300		
200 nm silica bead/40 nm silver	23.85	0.701	131.1	1.38
	167.0	0.299		
40 nm silica bead/40 nm silver	31.53	0.689	145.7	1.34
	188.1	0.311		
100 nm silica bead/40 nm silver	32.95	0.693	158.2	1.37
	203.9	0.307		
400 nm silica bead/40 nm silver	32.74	0.711	157.5	1.18
	206.2	0.289		
600 nm silica bead/40 nm silver	38.66	0.707	152.2	1.53
	204.1	0.293		

Today, many assays are based on the use of nanoparticles to obtain brighter emission than a single fluorophore.[19] Hence, it is of interest to compare the brightness of these particles to a single $Ru(bpy)_3^{2+}$ molecule. This comparison can be made by dividing the intensity of dye-labeled bare bead by the interior number of $Ru(bpy)_3^{2+}$ per particle, and we estimate that the particles are at least 1000-fold brighter than a single $Ru(bpy)_3^{2+}$ molecule for the small size dye-labeled silver shell. We are currently working on metal shells with an optimal sized silica bead, in which the dyes can be induced more completely. We also expect that the total enhancement effect will depend on the fluorophore used in the core.

Conclusions

Monodispersed silica beads were synthesized by the Stöber method, and $Ru(bpy)_3^{2+}$ complexes were incorporated into the silica beads by physical absorption. The diameter of the silica beads was adjusted in a range of 40−600 nm by adding the amount of ammonium in the preparation. The silver shell was coated onto the silica bead layer by layer through a chemical reduction of silver nitrate using sodium citrate in water. The thickness of the metal shell was controlled in a range of 5−50 nm. It was noted that the emission spectrum became narrow relative to the bare bead when the metal shell was 20 nm and the emission intensity was enhanced with an increase of shell thickness, which was consistent with the theoretical predictions for the metal shells. The emission enhancement reached saturation at 40 nm and then decreased probably due to the absorption from the metal shell at wavelengths of excitation and emission of the dye. The maximal emission enhancement efficiency was found to decrease with an increase of silica bead size, which was explained by a reductive volume of effective EM enhancement field relative to the whole interior volume of the cavity. The lifetime of $Ru(bpy)^{2+}$ in the silica bead became shorter with an increase of silver shell thickness, supporting

our prediction that the fluorescence enhancement occurs through an increase of the intrinsic decay rate for the fluorophore near the metal surface. These nanoparticles show considerable promise for markers in biological sensing.

Acknowledgment. This research was supported by a grant from NIH, HG-02655, EB-00682, and NCRR, RR-08119.

References and Notes

(1) (a) Lakowicz, J. R. *Anal. Biochem*. **2001**, *298*, 1. (b) Lakowicz, J. R. *Anal. Biochem*. **2005**, *337*, 171. (c) Sinner, E. K.; Reuning, U.; Kok, F. N.; Sacca, B.; Moroder, L.; Knoll, W.; Oesterhelt, D. *Anal. Biochem*. **2004**, *333*, 216. (d) Bjerneld, E. J.; Foldes-Papp, Z.; Kall, M.; Rigler, R. *J. Phys. Chem. B* **2002**, *106*, 1213. (e) Kummerlen, J.; Leitner. A.; Brunner, H.; Aussenegg, F. R.; Wokaun, A. *Mol.* Phys. **1993**, *80*, 1031. (f) Sokolov, K.; Chumanov, G.; Cotton, T. M. *Anal. Chem.* **1998**, *70*, 3898. (g) Evanoff, D. D.; White, R. L.; Chumanov, G. *J. Phys. Chem. B* **2004**, *108*, 1522. (h) Kamat P. V. *J. Phys. Chem. B* **2002**, *106*, 7729.

(2) (a) Hayat, M. A., Ed. *Colloidal Gold: Principles, Methods, and Applications*; Academic Press: San Diego, CA, 1991. (b) Rosi, N. L.; Mirkin, C. A. *Chem. Rev.* **2005**, *105*, 1547. (c) He, L.; Musick, M. D.; Nicewarner, S. R.; Salinas, F. G.; Benkovic, S. J.; Natan, M. J.; Keating, C. D. *J. Am. Chem. Soc.* **2000**, *122*, 9071.

(3) (a) Gryczynski, I.; Malicka, J.; Shen, Y. B.; Gryczynski, Z.; Lakowicz, J. R. *J. Phys. Chem. B* **2002**, *106*, 2191. (b) Malicka, J.; Gryczynski, I.; Gryczynski, Z.; Lakowicz, J. R. *Anal. Biochem*. **2003**, *315*, 57.

(4) (a) Kreibig, U.; Vollmer, M. *Optical Properties of Metal Clusters*; Springer-Verlag: Berlin and Heidelberg, Germany, 1995. (b) Feldheim, D. L.; Foss, C. A. *Metal Nanoparticles. Synthesis, Characterization and Applications*; Marcel Dekker: New York, 2002.

(5) (a) Messinger, B. J.; von Raben, K. U.; Chang, R. K.; Barber, P. W. *Phys. Rev. B* **1981**, *24*, 649. (b) Quinten, M. *Appl. Phys. B* **2001**, *73*, 245. (c) Kneipp, K.; Kneipp, H.; Itzkan, I.; Dasari, D. R.; Feld, M. S. *Chem. Rev.* **1999**, *99*, 2957.

(6) (a) Kumbhar, A. S.; Kinnan, M. K.; Chumanov, G. *J. Am. Chem. Soc*. **2005**, *127*, 12444. (b) Bruzzone, S.; Malvaldi, M.; Arrighini, G. P.; Guidotti, C. *J. Phys. Chem. B* **2005**, *109*, 3807. (c) Hubert, C.; Rumyantseva, A.; Lerondel, G.; Grand, J.; Kostcheev, S.; Billot, L.; Vial, A.; Bachelot, R.; Royer, P.; Chang, S.-h.; Gray, S. K.; Wiederrecht, G. P.; Schatz, G. C. *Nano Lett*. **2005**, *5*, 615. (d) Millstone, J. E.; Park, S.; Shuford, K. L.; Qin, L.; Schatz, G. C.; Mirkin, C. A. *J. Am. Chem.* Soc. **2005**, *127*, 5312.

(7) (a) Zhang, J.; Malicka, J.; Gryczynski, I.; Lakowicz, J. R. *Anal. Biochem.* **2004**, *330*, 81. (b) Zhang, J.; Malicka, J.; Gryczynski, I.; Lakowicz, J. R. *J. Phys. Chem. B* **2005**, *109*, 8701.

(8) (a) Hao, E.; Li, S.; Bailey, R. C.; Zou, S.; Schatz, G. C.; Hupp, J. T. *J. Phys. Chem. B* **2004**, *108*, 1224. (b) Schelm, S.; Smith, G. B. *J. Phys. Chem. B* **2005**, *109*, 1689.

(9) (a) Santra, S.; Zhang, P.; Wang, K.; Tapec, R.; Tan, W. *Anal. Chem.* **2001**, *73*, 4988. (b) Harma, H.; Lehtinen, P.; Takalo, H.; Lovgren, T. *Anal. Chim. Acta* **1999**, *387*, 11. (c) Giunchedi, P.; Conte, U.; Chetoni, P.; Saettone, M. F. *Eur. J. Pharm. Sci.* **1999**, *9*, 1. (d) Adler, J.; Jayan, A.; Melia, C. D. *J. Pharm. Sci*. **1999**, *88*, 371.

(10) (a) Jackson, J. B.; Halas, N. J. *J. Phys. Chem. B* **2001**, *105*, 2743. (b) Pham, T.; Jackson, J. B.; Halas, N. J.; Lee, T. R. *Langmuir* **2002**, *18*, 4915. (c) Jiang, Z.-j.; Liu, C.-y. *J. Phys. Chem. B* **2003**, *107*, 12411. (d) Sun, Y.; Wiley: B.; Li, Z.-Y.; Xia, Y. *J. Am. Chem. Soc*. **2004**, *126*, 9399−9406.

(11) (a) Hirsch, L. R.; Jackson, J. B.; Lee, A.; Halas, N. J.; West, J. L. *Anal. Chem*. **2003**, *75*, 2377. (b) Nehl, C. L.; Grady, N. K.; Goodrich, G. P.; Tam, F.; Halas, N. J.; Hafner, J. H. *Nano Lett*. **2004**, *4*, 2355. (c) Wang, Y.; Xie, X.; Wang, X.; Ku, G.; Gill, K. L.; O'Neal, D. P.; Stoica, G.; Wang, L. V. *Nano Lett*. **2004**, *4*, 1689. (d) Alvarez-Puebla, R. A.; Ross, D. J.; Nazri, G.-A.; Aroca, R. F. *Langmuir* **2005**, *21*, 10504.

(12) (a) Limmer, S. J.; Chou, T. P.; Cao, G. *J. Phys. Chem. B* **2003**, *107*, 13313. (b) Sun, Y.; Wiley: B.; Li, Z.-Y.; Xia, Y. *J. Am. Chem. Soc*. **2004**, *126*, 9399. (c) Wang, H.; Tam, F.; Grady, N. K.; Halas, N. J. *J. Phys. Chem. B* **2005**, *109*, 18218. (d) Radloff, C.; Vaia, R. A.; Brunton, J.; Bouwer, G. T.; Ward, V. K. *Nano Lett*. **2005**, *5*, 1187. (e) Shi, W.; Sahoo, Y.; Swihart, M. T.; Prasad, P. N. *Langmuir* **2005**, *21*, 1610. (f) K. E.; Xu, X.; Bulcock, S. R.; Cortie, M. B. *J. Phys. Chem. B* **2005**, *109*, 21516.

(13) (a) Winkler, J. R.; Gray, H. B. *Chem. Rev.* **1992**, *92*, 369. (b) Balzani, V.; Juris, A.; Venturi, M.; Campagna, S.; Serroni, S. *Chem. Rev*. **1996**, *96*, 759. (c) Prashant V. Kamat *Chem. Rev.* **1993**, *93*, 267.

(14) (a) Milosavljevic, B. H.; Meisel, D. *J. Phys. Chem. B* **2004**, *108*, 1827. (b) Glomm, W. R.; Volden, S.; Sjoblom, J.; Lindgren, M. *Chem. Mater*. **2005**, *17*, 5512.

(15) Stober, W.; Fink, A.; Bohn, E. *J. Colloid Interface Sci.* **1968**, *26*, 62.

(16) (a) Enderlein, J. *Phys. Chem. Chem. Phys*. **2004**, *4*, 2780. (b) Enderlein, J. *Appl. Phys. Lett*. **2002**, *80*, 315.

(17) (a) Gryczynski, I.; Malicka, J.; Gryczynski, Z.; Lakowicz, J. R. *Anal. Biochem*. **2004**, *324*, 170. (b) Lakowicz, J. R. *Anal. Biochem*. **2004**, *324*, 153.

(18) Anson, F. C.; Blauch, D. N.; Saveant, J. M.; Shu, C. F. *J. Am. Chem. Soc*. **1991**, *113*, 1922.

(19) (a) Smith, A. M.; Gao, X.; Nie, S. *Photobiol. Photochem*. **2004**, *80*, 377. (b) Michalet, X.; Pinaud, F. F.; Bentolila, L. A.; Tsay, J. M.; Doose, S.; Li, J. J.; Sundaresan, G.; Wu, A. M.; Gambhir, S. S.; Weiss, S. S *Science* **2005**, *307*, 538.